INDERSCIENCE PUBLISHERS
Linking academia, business and industry through research

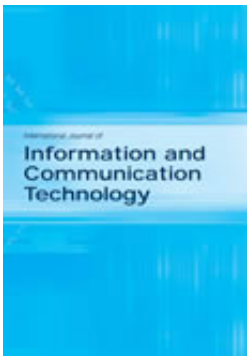

International Journal of Information and Communication Technology

ISSN online: 1741-8070 - ISSN print: 1466-6642
https://www.inderscience.com/ijict

Intelligent monitoring of icing condition of transmission lines based on intelligent vibration model

Ge Liu, Lin Guo, Shaolei Chen, Min Zhao, Fajun Li, Jing Zhang

Article History:

Received:	12 August 2024
Last revised:	11 November 2024
Accepted:	14 November 2024
Published online:	13 February 2025

Intelligent monitoring of icing condition of transmission lines based on intelligent vibration model

Ge Liu, Lin Guo* and Shaolei Chen

State Grid Sichuan Electric Power Company,
No. 366 Shuxiu West Road, Gaoxin District,
Chengdu City, Sichuan Province, China
Email: 19641218@163.net
Email: 11348585@qq.com
Email: chenslzju@163.com
*Corresponding author

Min Zhao

State Grid Sichuan Electric Power Company
Information and Communication Company,
No. 16 Jinhui West Second Street, Gaoxin District,
Chengdu City, Sichuan Province, China
Email: 1107635945@qq.com

Fajun Li

State Grid Bazhong Power Supply Company,
55 Jiangbei Avenue, Bazhong City, Sichuan Province, China
Email: lifajun0910@126.com

Jing Zhang

State Grid Yibin Electric Power Supply Company,
No. 17, Middle Section of Changjiang Avenue,
Xuzhou District, YiBin City, Sichuan Province, Chengdu, China
Email: 1010955792@qq.com

Abstract: Icing will not only increase the weight of the conductor to make the conductor bear greater vertical gravity and make the axial tension greater when the conductor gallops, but also increase the cross-sectional area of the conductor to increase the aerodynamic force of the conductor. Starting from the basic principles of distributed optical fibres and measurable physical quantities, this paper uses the method of combining theoretical analysis and simulation modelling to establish the mathematical and physical models and signal characteristic models of the multi-dimensional physical quantities (temperature, strain, vibration and light polarisation state) of distributed optical fibre monitoring and line icing and wind vibration events. Moreover, this paper constructs a multi-parameter distributed optical fibre sensing system according

to the monitoring requirements, which solves the problem of low signal-to-noise ratio in long-distance monitoring. Finally, through experimental verification, it is found that the model proposed in this paper has a good intelligent monitoring effect on the icing status of transmission lines, which can provide a reference for real-time monitoring of transmission lines.

Keywords: vibration model; transmission lines; icing; intelligent monitoring.

Reference to this paper should be made as follows: Liu, G., Guo, L., Chen, S., Zhao, M., Li, F. and Zhang, J. (2025) 'Intelligent monitoring of icing condition of transmission lines based on intelligent vibration model', *Int. J. Information and Communication Technology*, Vol. 26, No. 3, pp.47–71.

Biographical notes: Ge Liu obtained his PhD in Physics Electronice from University of Electronic Science and Technology of China. He currently works at Electric Power Dispatching and Control Center of State Grid Sichuan Electric Power Company as a Professor Senior Engineer. He is dedicated to the technology research, planning, design, construction, and maintenance of the company's communication network and selected as an expert judge of the Ministry of Science and Technology of the People's Republic of China.

Lin Guo obtained her Master's in Information and Communication Engineering from Chengdu University of Technology. She currently works at State Grid Electric Power Company Information and Telecommunication Company. Her research focuses on power communication technology.

Shaolei Chen obtained his PhD in Information and Communication Engineering from Zhejiang University. He is currently works at Electric Power Dispatching and Control Center of State Grid Sichuan Electric Power Company. His research focuses on power system and communication technology.

Min Zhao obtained her Master's in Signal and Information Processing from Sichuan University. She currently works at State Grid Sichuan Electric Power Company Information and Communication Company. Her research focuses on power communication technology.

Fajun Li obtained his Master's degree in Electronic and Communication Engineering from Chongqing University of Posts and Telecommunications. He currently works at State Grid Bazhong Power Supply Company. His research focuses on power communication technology.

Jing Zhang obtained his Master's degree in Electronics and Communication Engineering from Sichuan University. He currently works at State Grid Yibin Electric Power Supply Company. His research focuses on power communication technology.

1 Introduction

Under the action of wind load, transmission lines are excited to produce low-frequency and large-scale self-excited vibration. This kind of vibration of transmission line is called galloping, and the large-scale galloping of transmission line mainly occurs in the vertical direction, which will cause damage to the transmission system. In winter, transmission lines are easy to be covered with ice, and the icing of transmission lines will not only

increase the gravity of transmission lines, but also cause the cross section of transmission lines to become asymmetrical. Moreover, icing is an important cause of transmission line galloping, and it is also a difficult problem to solve. Long-term large-scale vibration causes variable tension of transmission lines, resulting in loose bolts, broken rings of fittings, broken transmission lines, and collapse of transmission towers. At the same time, it causes the interruption of transmission system operation and causes huge losses to people's lives and property, so the research on the stability of transmission lines has important engineering significance (Zhang et al., 2023).

Icing makes the cross-section of the conductor become asymmetrical, changes the aerodynamic characteristics of the conductor, produces negative damping effect, accumulates energy, and easily excites the conductor to gallop. In addition, icing is an important cause of transmission line galloping, and it is also an unavoidable phenomenon in practical projects. In the field of transmission line galloping research, icing has always been a difficult problem to solve (Li et al., 2023).

Transmission line engineering is an important project of national economic development. Nowadays, the production of all walks of life is inseparable from electric energy. The normal operation of transmission lines ensures the supply of electric energy and provides energy for production. Transmission lines have become non-circular cross-section structures due to weather, environment or self-aging problems, and conductors are long-span flexible structures, which are prone to galloping under the action of external transverse wind. The vibration of transmission lines with high flexibility is a typical nonlinear vibration. Moreover, transmission line structure has the characteristics of large flexibility, small damping and small mass. Its longitudinal scale is far larger than transverse scale, and it has axial one-way stiffness, so it can only bear tensile stress, but not compressive stress. Transmission line galloping often occurs at multiple degrees of freedom at the same time, which will cause coupled vibration in horizontal, vertical and torsional directions, and makes the study of transmission line stability more complicated. In addition, the coupled vibration of multiple degrees of freedom also makes the excitation energy transfer between degrees of freedom, making the transmission line more likely to gallop.

The existing online monitoring equipment for transmission lines mainly includes video monitoring equipment, tension sensors, micro meteorological sensors, and temperature sensors. These electronic sensors have disadvantages such as poor power supply reliability, insufficient monitoring range, and susceptibility to weather effects, making it difficult to meet the current high reliability and long-distance monitoring requirements. Fibre optic sensing technology monitors physical quantities such as temperature, strain, vibration frequency, and electric field strength of optical fibres by detecting characteristic parameters such as phase, intensity, polarisation state, and frequency of transmitted light. It has the advantages of high sensitivity and no need for power supply. According to the monitoring method, fibre optic sensors can be divided into point type and distributed type. Point type fibre optic sensors mainly use fibre Bragg gratings for monitoring, and the physical quantities that can be monitored mainly include temperature and strain. If a large range needs to be monitored, multiple sensors need to be arranged to form a sensing array. Therefore, using this method to monitor overhead transmission lines requires high installation costs and limited monitoring distance.

This article starts with the basic principles of distributed optical fibres and measurable physical quantities. Using theoretical analysis and simulation modelling methods, a

mathematical and physical model and signal characteristic model of the measurable multidimensional physical quantities (temperature, strain, vibration, and optical polarisation state) of distributed optical fibres and line icing, wind vibration, and lightning strike events are established. A multi parameter distributed optical fibre sensing system is constructed according to monitoring requirements, which solves the problem of low signal-to-noise ratio in long-distance monitoring. Through experiments, it is confirmed that the system can effectively monitor the icing, wind vibration, and lightning strikes of transmission lines.

The purpose of this paper is to use intelligent vibration model to monitor the icing status of transmission lines, and to provide reference for real-time monitoring of transmission lines. Based on the detectable parameters of multi-parameter distributed optical fibres, the effectiveness of monitoring wind speed, galloping and breeze vibration using distributed optical fibres is analysed and verified in this paper. The simulation results show that the vibration frequency can be reflected by analysing the strain changes inside the cable, and it is feasible to use distributed optical fibre to monitor galloping and breeze vibration.

2 Related works

2.1 Ice covered state

The study of aerodynamic characteristics of iced conductors is the basis for exploring the galloping stability and dancing response characteristics of transmission lines. Therefore, scholars at home and abroad have conducted extensive research on the aerodynamic characteristics of iced conductors based on wind tunnel tests, attempting to reproduce the actual shape of ice and measure the aerodynamic coefficients of conductors in wind tunnels. However, due to the diverse forms and shapes of ice cover, there are significant differences. In order to facilitate scientific and systematic research.

At present, ice cover is generally classified into several typical geometric shapes, with the most common being D-shaped, crescent shaped, and fan-shaped. Wang et al. (2023) measured the aerodynamic coefficients of single conductor, triple bundle, and quadruple bundle conductors based on wind tunnel test systems, and explored the static and dynamic aerodynamic characteristics of iced conductors; furthermore, further research has been conducted on the dancing stability of extra thick ice covered conductors, and some of the research results have been applied to the anti dancing design of transmission lines. Chen et al. (2020b) studied the aerodynamic characteristics of six different types of quasi elliptical iced conductors, and discussed the effects of turbulence, wind attack angle, ice saturation, ice thickness, and other factors on the aerodynamic characteristics of conductors, as well as the general rules of galloping stability of quasi elliptical iced conductors. As scholars further improve their understanding of the aerodynamic characteristics of wires, the trend of related research is towards increasing the number of splits and paying more attention to the aerodynamic forces of each sub wire.

2.2 Ice covered conductor dancing model

Ice covered conductor dancing is a nonlinear self-excited vibration, and its dancing characteristics are not only related to its own structural parameters, but also closely

related to the aerodynamic force of the conductor after being covered with ice. Foreign researchers have conducted extensive basic research on this special form of conductor vibration, dancing. Han et al. (2022) derived an approximate analytical solution for the fluctuation of vertical amplitude with wind speed in the case of only considering vertical single degree of freedom for the dancing model of iced conductors. The solution was compared and verified with wind tunnel test results and observation results of real transmission line dancing response.

As research progresses, scholars gradually realise that in actual transmission lines, vertical and horizontal dancing usually occur simultaneously. Therefore, a dancing model that only considers vertical degrees of freedom is limited and cannot accurately reflect the motion characteristics of actual iced conductor dancing. Wang et al. (2024) analysed the dancing response characteristics of iced conductors using a two degree of freedom linear vibration model coupled vertically and horizontally. It was theoretically proven that horizontal vibration has a significant impact on dancing, and horizontal vibration cannot be ignored in dancing stability analysis. Wang et al. (2020) obtained the relaxation stability domain and vibration response of a two degree of freedom model coupled vertically and horizontally for blunt body structures with triangular and elliptical cross-sections through wind tunnel tests. The effects of wind speed, wind attack angle, and Reynolds number on flutter were systematically studied.

Scholars have gradually noticed that torsional turning vibration is also an important part that cannot be ignored in the dancing process, so the two degree of freedom dancing model coupled with vertical and torsional turning quickly became the focus of researchers. Zhang et al. (2020) proposed a two degree of freedom dancing model with vertical and torsional coupling, where the elastic axis does not coincide with the centre of mass. Based on this model, the critical condition for bifurcation was proposed, and the possible periodic solutions during the wire dancing process were also obtained. Shen et al. (2023) analyses the effects of structural (initial tension, line density, mass per unit length, damping ratio) and environmental (wind speed, incoming flow density, ice thickness, initial wind attack angle) parameters on the dancing wind speed and dancing characteristics based on a two degree of freedom model considering the coupling of vertical and torsional directions of conductors, using multi-scale and numerical methods, and discusses the complex motion forms that may be caused by torsional vibration bifurcation.

2.3 Ice cover monitoring and warning

Sun et al. (2021) installed high-definition cameras on transmission line towers to detect real-time images of the lines. Digital image processing technology was used to track contours, extract contours, and perform pre-processing operations. The images were then analysed to determine the amplitude of wire dancing based on changes in position. He et al. (2024) proposed an embedded dance monitoring system that uses cameras to capture the working images of wires, transmits the images to a computer for processing, and calculates the angle changes between the wires and the iron tower through the computer. When the calculation result exceeds the safety threshold, an alert is issued.

Acceleration sensor technology is the installation of acceleration sensors at multiple locations on transmission lines. The sensors follow the movement of the wires and record the acceleration changes at multiple points on the wires. The computer integrates the

acceleration information and obtains data such as the speed and displacement of the line dancing through integration and other methods, thereby detecting the operation of the wires. Brettschneider and Fofana (2021) developed an online dance detection system using an accelerometer to measure line dance caused by uneven ice cover, and transmitted the measured data to the host using a GSM module for data analysis; this method can detect the dancing acceleration and displacement changes of transmission lines and issue warnings. However, this method does not take into account the component acceleration error caused by wire torsion. Huang et al. (2020) used a nine axis sensor to correct the torsional acceleration of the wire, and successfully calculated the operation of the entire transmission line using data obtained from multiple nine axis sensors in linkage. The error in the swing amplitude can reach 10% of the swing amplitude. When the swing amplitude of the wire increases, the corresponding absolute value of the error will also increase.

Zhou et al. (2023) used AutoCAD for model preprocessing and GAMBIT for subsequent processing to establish a dry growth ice cover prediction model; Dong et al. (2022) used CFD to establish collision coefficient models based on fluid mechanics and freezing coefficient models based on thermodynamics, analysed the relationship between the two models and environmental parameters, and finally verified the correctness of the simulation results through experiments in an artificial climate chamber; Yang et al. (2023) used ABAQUS to simulate the icing situation of a transmission line in Shaoguan, and conducted a detailed study on the influencing factors of environmental temperature, humidity, and wind speed during the icing process of the transmission line; Yang et al. (2022) established a flow field model for power transmission lines based on the standard turbulence model of gas-liquid two-phase flow, and studied the influence of factors such as ice cover shape and wind attack angle on collision coefficient; Chen et al. (2020a) simulated the flow field characteristics around insulators during the icing process, analysed the motion characteristics of water droplets in the flow field, and established an icing prediction model for insulator wet growth based on thermodynamics and energy conservation laws; Ciesielka et al. (2020) used GAMBIT to establish a model of LGJ-210/25 steel core aluminium stranded wire, studied the influencing factors of collision process during transmission line icing, and established a prediction model for transmission line icing by improving the calculation accuracy of freezing coefficient; Ma et al. (2022) used FLUENT to simulate the collision characteristics of water droplets on transmission lines, determined the freezing coefficient model of transmission lines from the thermal equilibrium equation, and proposed a calculation model for key parameters during the growth process of transmission line icing by combining the Makkonen model and icing monitoring data.

3 Wind vibration monitoring and analysis

3.1 Galloping monitoring analysis

In winter, due to the irregular icing of the line, the lift force is unbalanced, which easily leads to the line galloping. The possible vibration directions of the galloping are transverse, longitudinal and torsional. The three-degree-of-freedom model of the ice-covered wire galloping is shown in Figure 1, which θ is the torsional angle of the line.

Figure 1 Galloping model of icing conductor

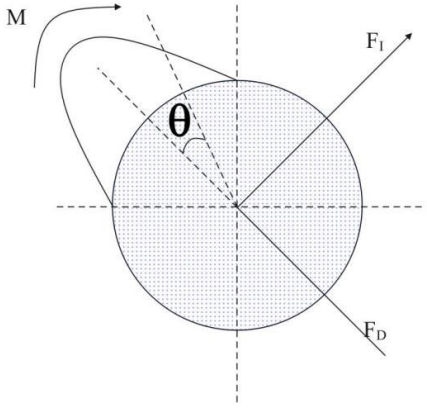

However, the solution of the three-degree-of-freedom model equation is very complicated. In order to simplify the calculation of the torsional degrees of freedom ignored in this paper, the two-degree-of-freedom equation listed is shown in formula (1) (Huang et al., 2023):

$$\begin{cases} (m_0+m_i)\dfrac{d^2z}{dt^2}+C_z\dfrac{dz}{dt}+T\left(\dfrac{k_w\pi}{L}\right)^2 z=(m+m_i)g+F_L\cos\alpha_1-F_D\sin\alpha_1 \\ (m_0+m_i)\dfrac{d^2x}{dt^2}+C_x\dfrac{dx}{dt}+T\left(\dfrac{k_w\pi}{L}\right)^2 x=F_L\sin\alpha_1-F_D\cos\alpha_1 \\ F_L=\dfrac{1}{2}\rho_a V^2 B_t C_L \\ F_D=\dfrac{1}{2}\rho_a V^2 B_t C_D \end{cases} \tag{1}$$

In the formula, m_0 is the linear density of OPGW, m_i is the icing mass of OPGW, C_z and C_x are the damping coefficients in the two vertical directions respectively, T is the conductor tension, and L is the line gap. k_w is the galloping order, C_L and C_D are the lift coefficient and drag coefficient respectively, ρ_a is the air density, V is the wind speed, B_t is the characteristic length of the iced conductor cross section, B_t is the cable lift, and F_D is the cable resistance.

This equation is a bivariate quadratic partial differential equation, and it is difficult to obtain its analytical solution in mathematics. In engineering, if we want to get the galloping trajectory, we usually use the numerical solution method. This paper uses the ODE45 module of MATLAB to solve it numerically. The specific line parameters are as follows: m = 1.5 kg, m_i = 0.55 kg, l = 300 m, C_z = 0.08, C_x = 0.05, T = 148 KN, B = 0.25 m and v = 10 m/s.

Figure 2(a) shows the calculated track of the ice-covered galloping of the line. When the line gallops, the amplitude in the longitudinal direction (vertical ground direction) accounts for the main part, and the lateral direction is only about 1/10 of the longitudinal direction. Therefore, the galloping situation can be estimated by estimating the vibration frequency in the longitudinal direction when galloping. The galloping longitudinal component FFT is decomposed to a frequency of 0.48 Hz, as shown in Figure 2(b), so the

frequency monitoring range of the distributed optical fibre to monitor the galloping of the cable should be at least less than 0.5 Hz.

Figure 2 Time-domain and frequency-domain curves of the line obtained from numerical simulation, (a) time domain curve (b) frequency domain curve (see online version for colours)

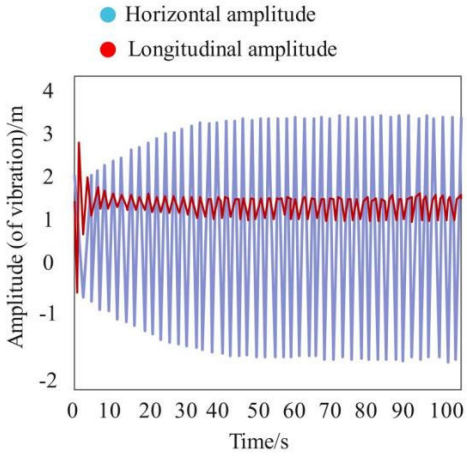

(a)

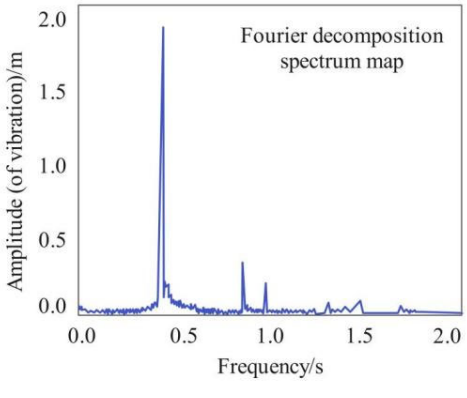

(b)

Transmission line galloping occurs only when irregular icing produces unbalanced lift. According to the parabola method and Hooke's law of elastic deformation, the change of horizontal tension caused by galloping can be calculated by formula (2):

$$\Delta T_0 = \frac{E_y \times S\Delta l}{L_S} = \begin{cases} \dfrac{n_w^2 \pi^2 E_y S a_0^2}{4 l L_S} \sin^2 \omega_l t, & n_w = even \\ \dfrac{n_w^2 \pi^2 E_y S a_0^2}{4 l L_S} \sin^2 \omega_l t - \dfrac{2 g_m l E_y S a_0}{n \pi \sigma_n L_S \cos \beta} \sin \omega_l t, & n_w = odd \end{cases} \tag{2}$$

Among them, ΔT_0 is the change of horizontal tension, E_y is the Young's modulus of OPGW, Δl is the change of the length of the line when galloping, ω_l is the galloping frequency, a_0 is the amplitude of galloping, and n_w is the half-wave number of galloping. The common half-wave observation number is 1, 2, 3, 4, and the amplitude of more than 5 half-waves is too small, and the accident of transmission line can be ignored.

Table 1 Galloping simulation line parameters

Parameter	*S*	*E*	*Ls*	*RTS*	*G0*
Unit	mm^2	105 N/mm^2	m	kN	kg/m
Numeric value	629.31	1.29	1,038	353.21	2.734

The simulation results are shown in Figure 3. The results show that when the line gallops, the stress at the suspension point changes periodically with the vibration. Although the Brillouin scattering module can monitor the stress change of the cable, due to the weak Brillouin backscattering signal, it is necessary to average the collected signal information many times. Long-distance monitoring often takes tens of seconds to several minutes, so it is difficult to monitor the stress changes at the galloping place. The OTDR module can generally monitor the vibration from a few to tens of Hz. By analysing the frequency spectrum of the vibration signal, the vibration frequency and vibration situation of the galloping can be monitored. The vibration at the suspension point on the vibration intensity spectrum should be more intense. Moreover, because its stress is relatively concentrated, it is feasible to use distributed optical fibre to monitor cable galloping.

Figure 3 Variation of horizontal tension under different half waves (see online version for colours)

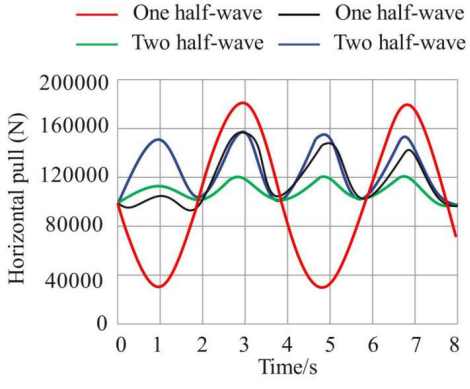

3.2 Breeze vibration monitoring and analysis

When the breeze vibration is stable, the power of the wind load and the self-damping power of the cable will be balanced, as shown in formula (3) (Weng et al., 2021).

$$P_W = P_D \tag{3}$$

In formula, P_W is the wind load power, and P_D is the self-damping power of the cable.

The displacement of the cable when the breeze vibrates is as shown in formula (4).

$$y = A_0 \cos\left(\omega_w t - \varphi_w\right) \tag{4}$$

In the formula, A_0 is the amplitude of the vibration, ω_w is the angular frequency of the lift, and φ_w is the phase difference between the lift and the displacement. The wind input power can be calculated by formula (5), and the simplified result is shown in formula (6).

$$P_W = \frac{2}{t}\int_0^{\frac{T}{2}} \left\{ F_y \sin\omega t \frac{d\left[A_0 \cos\left(\omega_w t - \varphi_w\right)\right]}{dt} \right\} dt \tag{5}$$

$$P_W = \pi F_y A_0 f_m = \frac{1}{2} C_L \rho V^2 d_l \pi A_0 f_m \tag{6}$$

In the formula, f_m is the vibration frequency of the cable under the Karman vortex, d_l is the diameter of the cable, $A_0 = \eta d_l$ and η is a constant. The expression is shown in formula (7).

$$P_W = 51.342 C_L \eta f_m^3 d_l^4 \tag{7}$$

The formula of wind energy input power obtained by fitting is as shown in formula (8).

$$\begin{cases} P_W = \left(y/d_l\right) 2^{a_1+a_2} e^{a_3} f_m^3 d_1^4, \left(y \le 0.6 d_l\right) \\ P_W = 27.513 f_m^3 d_1^4, \left(0.6 d_l < y < d_l\right) \end{cases}$$

$$\begin{cases} P_W = \left(y/d_l\right) 2^{a_1+a_2} e^{a_3} f_m^3 d_1^4, \left(y \le 0.6 d_l\right) \\ P_W = 27.513 f_m^3 d_1^4, \left(0.6 d_l < y < d_l\right) \\ P_W = 0, \left(y > d_l\right) \end{cases} \tag{8}$$

Among them, $a_1 = 0.0519$, $a_2 = 1.4124$ and $a_3 = 4.0125$.

The cable self-damping power expression is shown in formula (9).

$$P_D = \frac{\pi}{2} l_i h_D y^2 f_m^4 T^{-1.5} m_0^{1.5} \tag{9}$$

Among them, l_i is the line pitch, h_D is the cable hysteresis damping coefficient, T is the tension force on the cable, and m_0 is the cable gear length mass. After substituting the above formula into the power calculation equation (3), the formula (10) can be deduced:

$$(y/d) 2^{a_1+a_2} e^{a_3} f_m^3 d^4 = \frac{\pi}{2} l_i h_D y^2 f_m^4 T^{-1.5} m_0^{1.5} \tag{10}$$

In the setting of simulation line parameters, the span l is 220 m, the weight per unit length is 0.9743 kg/m, the tension force is 72,300 N, and the cross-sectional area is 277.75 mm^2. The time-domain curves of breeze vibration at different wind speeds of 2 m/s, 2.5 m/s, 3 m/s, 5 m/s and 10 m/s are shown in Figure 4. The vibration frequencies are 21.3 Hz, 26.6 Hz, 31.9 Hz, 53.2 Hz and 106.4 Hz respectively, and the smaller the diameter of the cable, the greater the vibration frequency. Generally speaking, the range of breeze vibration is in the range of 20~200Hz, so it is necessary to monitor the breeze vibration of the cable. The frequency monitoring range is greater than 110Hz, and when the wind speed is greater, the increase of cable self-damping is greater than the amplitude of wind input power, so the higher the frequency of breeze vibration and the smaller the

amplitude, the more difficult it is to monitor breeze vibration with distributed optical fibre than galloping.

Figure 4 Time-domain diagram of cable breeze vibration at different wind speeds obtained by simulation (see online version for colours)

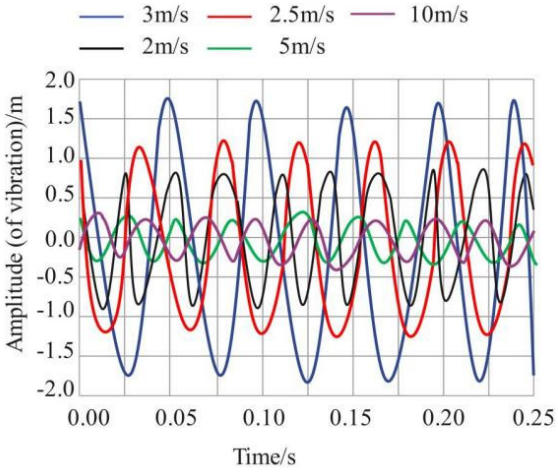

3.3 Sensor performance parameters

In order to realise the whole line monitoring of overhead transmission lines, the sensing distance of the equipment must be at least greater than 60 km, and if the output light power is simply increased, it may cause nonlinear scattering effects such as stimulated Raman scattering and stimulated Brillouin scattering. Therefore, the centralised and distributed Raman amplification technology of EDFA is used in this paper to avoid this phenomenon. The distributed Raman amplification technology is based on the stimulated Raman scattering effect. Its main principle is that when two Stokes-spaced light are injected into the fibre. At the same time, if the frequency difference between them is within the Raman gain spectrum of the fibre, the intensity of the light with a longer wavelength will increase, and the intensity of the light with a shorter wavelength will decrease. Therefore, the signal light can be amplified by adjusting the pump frequency of the Raman amplifier appropriately to improve the system performance. The Brillouin sensor module and the phase-sensitive Rayleigh scattering module of the device both use coherent monitoring methods to improve signal strength and signal-to-noise ratio. The coherent detection principle of the phase-sensitive Rayleigh scattering module is introduced below.

The Rayleigh backscatter signal light field in the optical fibre is shown in formula (11):

$$E_S(t) = E_b(t)\exp j\left[2\pi\omega_S + \varphi_S(t)\right] \tag{11}$$

The light field of light is shown in formula (12):

$$E_L(t) = E_1(t)\exp j\left[2\pi\omega_L + \varphi_L(t)\right] \tag{12}$$

In the formula, $E_S(t)$ and $E_L(t)$ are the amplitudes of the Rayleigh scattering signal light field and the local oscillator light field respectively, ω_S and ω_L are the amplitudes of the signal light and the reference light respectively, and $\varphi_S(t)$ and $\varphi_L(t)$ are the phases of the signal light and the reference light respectively. After the two are coherent, they enter the photodetector, and the intermediate frequency component after the coherence can be expressed as formula (13).

$$i_{ac}(t) = 2\beta E_1(t)\cos[\theta(t)]\cos[2\pi\Delta ft + \Delta\varphi(t)] \tag{13}$$

Among them, β is the responsivity of the photodetector, $\theta(t)$ is the polarisation angle between the signal light and the reference light, ω_S and ω_L are the angle between the signal light and the reference light respectively, Δf is the frequency difference between the angle between the signal light and the reference light, and $\Delta\varphi = \varphi_S(t) - \varphi_1(t)$ is the phase difference between the two beams. When the light passes through the band-pass filter, most of the noise power can be filtered out, thereby improving the detection sensitivity.

The effective signal power of the heterodyne detection output is shown in formula (14).

$$P_c = 2\beta^2 P_{RS} P_{L0} R_L \tag{14}$$

In the formula, P_{RS} is the signal optical power, P_{L0} is the reference optical power, and R_L is the load resistance.

The effective signal power of the conventional direct detection is shown in equation (15).

$$P_0 = 2\beta^2 P_S^2 R_L \tag{15}$$

4 Models and experiments

4.1 Model design

The dance detection device is installed on the transmission line, and the working topology diagram of the dance detection spacer of the transmission line is shown in Figure 5. The comprehensive state detection spacer of the transmission line is installed between two transmission lines. The detection spacer is based on the principle of mutual inductance and obtains electricity through self induction to obtain the electrical energy of the line's excited magnetic field. One part is used for direct power supply, and the other part is used to store electrical energy in lithium titanate batteries. The interval rod for comprehensive status detection of transmission lines collects parameters such as motion acceleration, temperature, humidity, and current of the transmission lines. Using Bluetooth communication technology to transmit data to a reference station (positioning reference station) near the tower, which is installed at the tower leg of the tower. The reference station forwards data through the communication module and sends the data measured by the detection spacer to the power system network. The power system dedicated network is securely connected to the relay server through optical fibre, and the relay server performs operations such as decoding and encryption on the data of the

power system dedicated network. The relay server then transmits the data to the power grid company server through Ethernet.

Figure 5 Working topology diagram of the IoT monitoring system for transmission lines (see online version for colours)

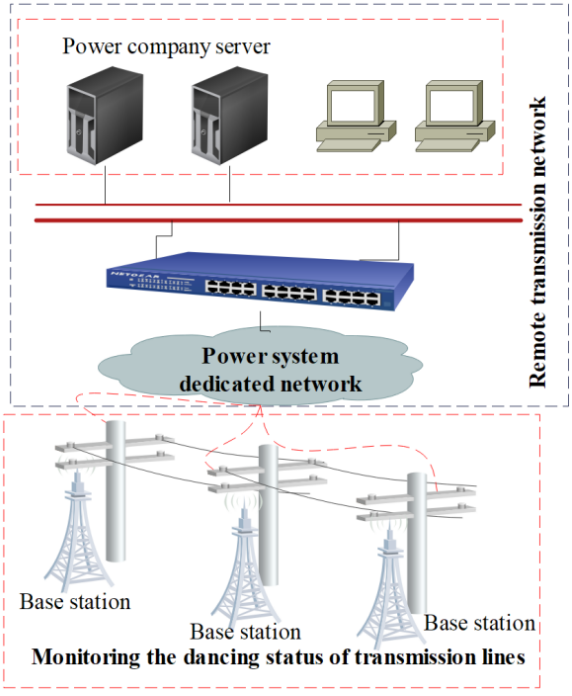

The STM32F401 is selected as the main control chip for the dance monitoring tower terminal, and the peripheral devices mainly include ZigBee communication module, Bluetooth mesh communication module, and 4G communication module. Therefore, it is necessary to design the corresponding module application circuit and interface with the minimum system. Regarding the ZigBee communication module ZA2530, it has been clarified that the ZigBee communication module on the dance monitoring tower terminal serves as the coordinator. Whether it is a terminal node or a coordinator, they are different working modes in software programs, and their hardware application circuits and MCU interface circuits are consistent.

The dance amplitude monitoring system subtracts 1,000 displacement data points collected on the X and Y axes from the standard displacement to obtain the difference between the two. Use MATLAB software. A transmission line dancing monitoring platform was designed using LabVIEW software, with the main purpose of obtaining the dancing acceleration, angular velocity, and amplitude of the wires during transmission line dancing.

A multi parameter distributed fibre optic system has been built, with three main units for the multi parameter distributed fibre optic host. The Brillouin sensing module and phase sensitive Rayleigh scattering module share one main unit, while the forward continuous light sensing host and slave are two main units, respectively. The host unit has built an operating system that allows for on-site and remote adjustment of host

parameters, including scanning range, scanning interval, sampling rate, sampling length, data accumulation times, circuit amplification coefficient, Raman amplification coefficient, pulse width, etc. It can also be displayed on an external display screen. In order to test the monitoring performance of multi parameter distributed fibre optic sensing and prove that it can meet the requirements of online monitoring of transmission lines, it is necessary to conduct vibration, temperature, stress, and polarisation state positioning experiments on this equipment to obtain the dynamic range, spatial resolution, and monitoring range of the multi parameter distributed fibre optic sensing system. The vibration performance testing experiment of distributed fibre optic sensing is shown in Figure 6.

Figure 6 Scheme diagram of vibration sensing test (see online version for colours)

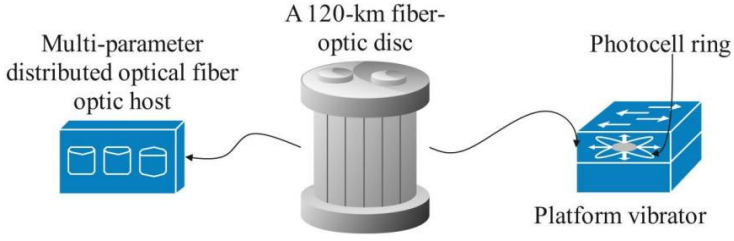

Figure 7 Transmission line monitoring system based on smart grid internet of things (see online version for colours)

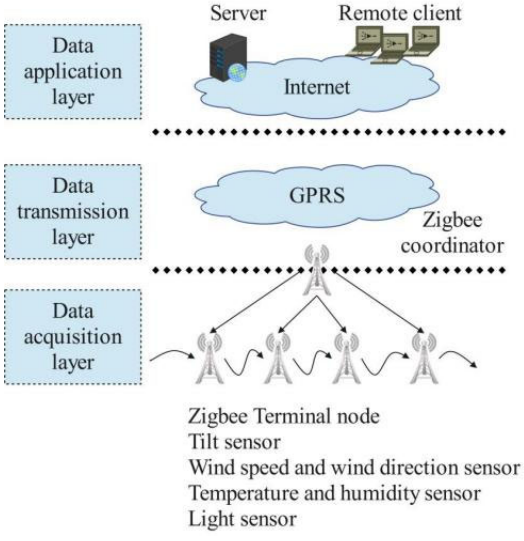

The application architecture of the smart grid IoT transmission line monitoring system is shown in Figure 7, which is divided from bottom to top into data acquisition layer, transmission layer, and application layer. This system mainly includes two modules: on-site multifunctional monitoring base station and monitoring centre software. The former is installed on the towers of transmission lines and powered by solar energy to collect and analyse real-time monitoring data and alarm information. The processed

monitoring data is transmitted to the GPRS module through the ZigBee wireless communication system, and then uploaded to the upper computer monitoring centre through the GPRS module. The ZigBee module aggregates on-site monitoring information and collects data on surrounding towers, eliminating the need to install GPRS modules on each tower and reducing cost expenditures. The GPRS module is an important medium for connecting the field and the upper computer. The monitoring centre communicates with the on-site multifunctional detection base station by transmitting instructions and obtaining real-time on-site monitoring data transmitted by the on-site monitoring terminal; simultaneously storing and managing various monitoring information, it can provide application services for remote customers of the system.

The sensor devices and monitoring nodes distributed in different nodes of the power system form a hardware platform together. At the same time, the method of combining short-distance communication transmission mode and long-distance communication transmission mode is used to effectively ensure the speed and stability of data. The establishment of the communication network provides a software platform for the comprehensive processing of data and the operation of the detection software. The schematic diagram of the structure of the system is shown in Figure 8.

Figure 8 System architecture (see online version for colours)

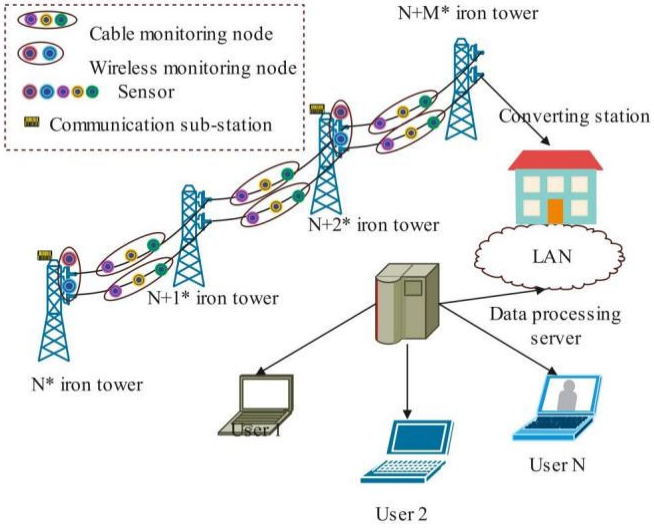

The laying technology of OPGW optical fibre requires the connection of OPGW optical cable every 5 kilometres. When the optical cable is connected, the optical fibre connection at both ends can only be located at the fusion point. This requires the use of optical fibre switching when building a communication network. To ensure the communication quality in the area, usually the arrangement range of wireless communication devices is based on the optical fibre contact as the centre line, and the radiation radius is within 2.5 km. In addition, the distance between OPGW optical cable continuation boxes is five kilometres, but the distance between towers of the actual transmission line or between monitoring points cannot be exactly equal to 5 kilometres, resulting in the following two situations as shown in Figure 9.

1 If the monitoring point has an OPGW junction box, the monitoring equipment will be installed there, and the transmission equipment will be connected to the optical cable.

2 If the monitoring point does not have an OPGW junction box, the signal of the monitoring point is collected and transmitted by WiFi wireless communication. The basic principle of wireless transmission at the junction box-free monitoring point is to access the data information to the client WAC through the network, and at the same time transmit the data to the WiFi wireless communication access point WAP, and then transmit the data to the junction box through the wireless bridge, the designated position of the box. Finally, the data is transmitted to the control centre through wired communication, that is, optical cable.

Figure 9 Networking mode (see online version for colours)

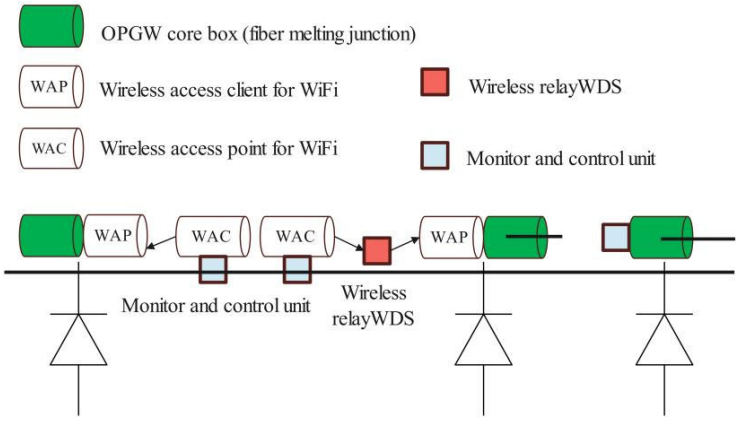

4.2 Test

4.2.1 Galloping simulation experiment

The galloping frequency of transmission lines ranges from 0.5 to 3 Hz. The galloping frequency is related to the structure, length and natural frequency of the line. At the same time, the strain value change inside the cable can reflect the frequency value of the cable when galloping. The experimental site set up to explore the multi-parameter distributed optical fibre sensing equipment to monitor the galloping of the OPGW actual line is shown in Figure 10.

When overhead transmission lines are covered with ice, the change of strain can be monitored on OPGW, and the ice thickness of transmission lines can be calculated by substituting the strain into the state equation of transmission lines. In order to test the ability of multi-parameter distributed optical fibre equipment to monitor the strain of OPGW line, the tensile force test of OPGW is carried out in the laboratory. The OPGW model used in the experiment is OPGW-96B1.3-150, the rated tensile strength (RTS) is 94.8 kN, and the length is 100m. Tensile forces of 15%, 60% RTS, 65% RTS, 85% RTS and 125% RTS are successively applied to test the frequency shift of BOTDR when OPGW is tensile, and the experimental settings are shown in Figure 11.

Figure 10 Schematic diagram of icing galloping experiment on transmission lines (see online version for colours)

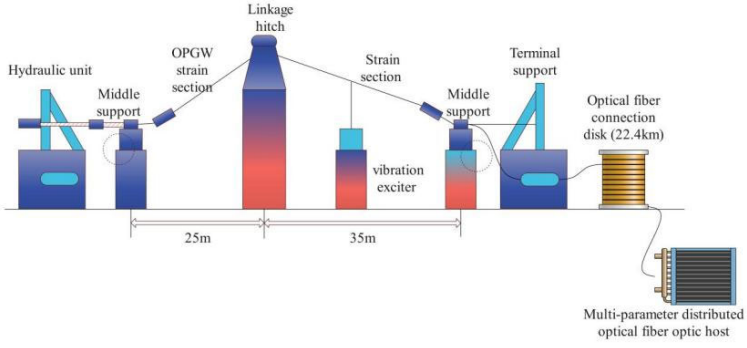

Figure 11 Stress-strain performance test device of OPGW (see online version for colours)

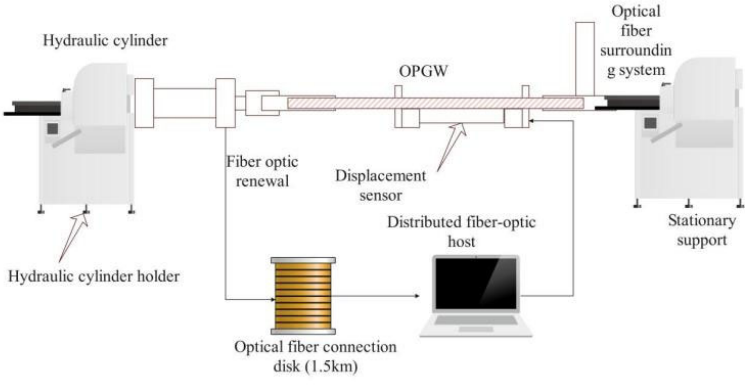

4.3 Results

The frequency shift data obtained from the frequency shift changes of the distributed optical fibre system under different tension forces are shown in Figure 12.

In order to get the galloping positioning signal, the time domain curve needs to be processed by moving average and difference at first. The so-called moving average is to select a window with a fixed length, carry out arithmetic average of the data in the window, and then move according to the time series. Every time the window slides, the front data will be removed and the last data will be replaced, and then a new filtered data sequence will be obtained. The moving average algorithm is equivalent to low-pass filtering, which can eliminate high-frequency noise. Among them, the selection of the sliding window is very important. To ensure both noise suppression and signal integrity, the sliding average window is taken as 20 units in this paper. Differential processing is to subtract two adjacent sets of data as a new set of data. The vibration intensity-distance diagram after differential treatment is shown in Figure 13.

Figure 12 Variation of frequency shift under different tensile forces (see online version for colours)

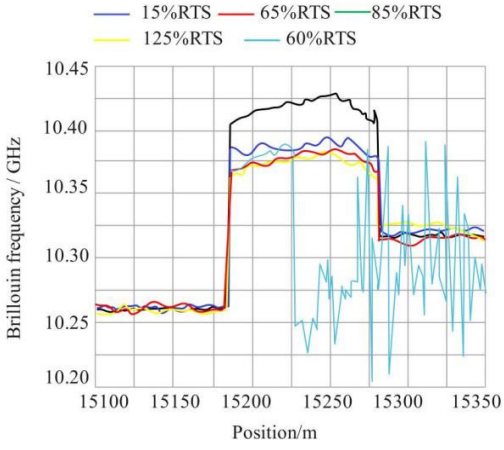

Figure 13 Vibration intensity-distance diagram after differential processing, (a) differential diagram of galloping data with an external fibre length of 22.4 km (b) differential diagram of galloping data with an external fibre length of 59.6 km (see online version for colours)

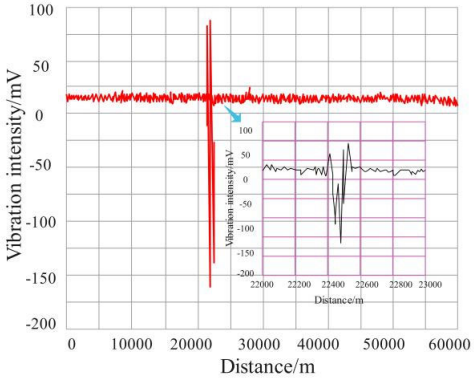

(a)

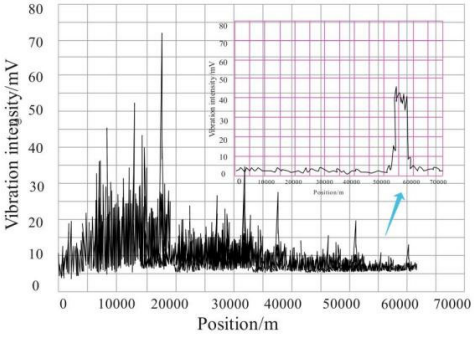

(b)

Figure 14 Three-dimensional image of position-frequency-amplitude of line galloping, (a) three-dimensional diagram of galloping frequency domain for an external 22.4 km optical fibre disk (b) three-dimensional diagram of galloping frequency domain for an external 59.6 km optical fibre disk (see online version for colours)

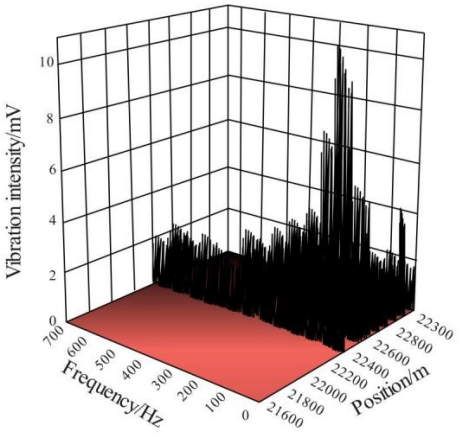

(a)

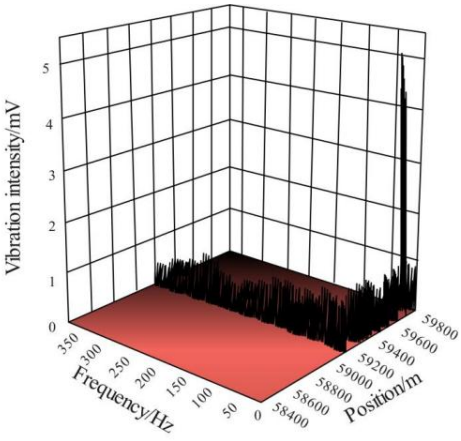

(b)

The three-dimensional diagram of position-frequency-amplitude when the cable gallops is shown in Figure 14. It can be seen that when the cable gallops, there will be a peak value in the frequency domain in the galloping area, and the peak value is concentrated in the low frequency range. This can be used as a criterion to identify the cable galloping.

The time-vibration intensity curves at the galloping positioning position obtained by external 22.35 km and 58.62 km optical fibre disks are extracted and fast Fourier changes are performed. It should be noted that if a group of data is directly used for Fourier decomposition, the frequency resolution is 754/4,096 = 0.18 Hz, which cannot meet the low-frequency monitoring requirements of galloping. Therefore, it is necessary to splice several consecutive sets of monitoring data to obtain sufficient frequency resolution. In this paper, 8 consecutive sets of data are selected for splicing according to the needs, and

the frequency resolution is 0.02 Hz to meet the monitoring requirements. The resulting spectrogram is shown in Figure 15.

Figure 15 Spectrum analysis of galloping experiment, (a) galloping spectrum at 22,560 m (b) Galloping spectrum at 59,600 m (see online version for colours)

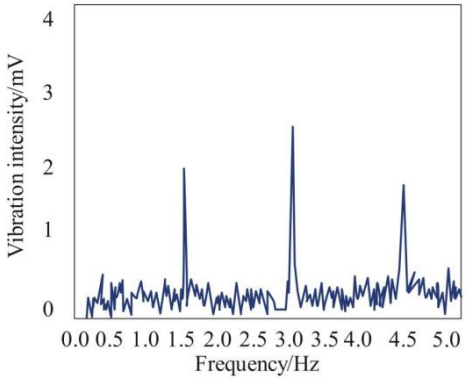

(a)

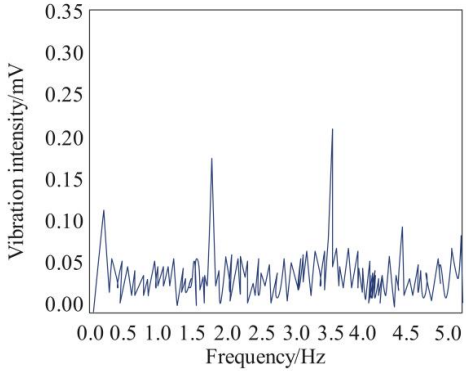

(b)

Table 2 System performance test results

	Accuracy (%)	*RMSE*	*Response time (ms)*
Edge computing (Zhang et al., 2020)	84.616	0.443	238.746
Deep belief networks (Shen et al., 2023)	84.602	0.458	257.997
BOTDR temperature monitoring (Sun et al., 2021)	74.596	0.598	196.803
Machine learning sensor networks (He et al., 2024)	73.806	0.604	258.327
Ultrasonic testing (Yang et al., 2023)	65.668	0.603	209.382
GS-XGBoos (Ma et al., 2022)	72.585	0.319	270.180
Model in this article	98.343	0.014	123.412

To further validate the system performance of the model proposed in this article, simulation experiments were conducted in MATLAB, and indicators such as accuracy,

root mean squared error, and system response time were used as experimental indicators to quantify the performance of the monitoring system. By inputting historical data and obtaining simulation monitoring results, comparing the simulation results with the actual results, the experimental results shown in Table 2 are obtained.

4.4 Analysis and discussion

As shown in Figure 12, when an optical fibre disk of about 15 km is connected before the OPGW, the relationship between micro-strain and frequency shift is 19.37 ± 0.427 με/MHz in the 15,180–15,280 m segments. With the increase of tension, the frequency shift value of OPGW segment obtained by BOTDR also increases. At this time, the remaining length of the fibre is basically consumed and the strain value appears. The tension at 60% RTS is basically the same as that at 15% RTS. The reason is that the remaining length of the optical fibre inside the optical cable has not been consumed. The average OPGW strains of 65% RTS and 85% RTS are 223.52 με and 865.45 με. Generally speaking, the remaining length of the optical fibre can only be consumed when the tensile force reaches 60% RTS of the maximum tensile stress of OPGW. At this time, by continuing to increase the tension force, the force situation of the line can be monitored to evaluate the icing of the line. When the tension force is 125% RTS, the line is pulled off, and the frequency shift value changes greatly at this time. From the experimental results, it is often difficult to monitor the strain of the line when the icing on the line is very slight. When the equipment starts to monitor the strain of the line, the icing on the line is often serious. Therefore, the equivalent thickness of the icing on the line can be used to evaluate the situation when the icing on the line is relatively serious.

As shown in Figure 13, since only the OPGW galloping area vibrates, and the vibration intensity of most areas is random white noise, the position-vibration intensity curve can be obtained by subtracting it after averaging. It can be seen from the figure that when the distance of the external optical fibre is 22.35 km, the galloping position obtained after difference is relatively clear, and the galloping position can be easily located. However, when the length of the external optical fibre is 58.62 km, due to the serious attenuation of the backscattered light, the signal-to-noise ratio of the galloping position obtained after difference and sliding average is relatively low. According to the information in the figure, the galloping position is consistent with the position of the OPGW galloping section. This verifies that the intelligent monitoring model for icing status of transmission lines proposed in this article has high monitoring accuracy and good monitoring effect on the impact of harsh external environments on transmission lines.

As shown in Figure 14, when the external 22.35 km optical fibre disk line gallops, its spectral diagram will have a peak vibration intensity near 1.41 Hz and its frequency doubling (2.82 Hz, 4.23 Hz), and when the external 58.62 km optical fibre disk line gallops, its spectral diagram will have a peak vibration intensity near 1.62 Hz and its frequency doubling (3.24 Hz), which is the same as the vibration frequency set in the experiment. It proves that the device can accurately monitor the galloping frequency of the line, and its frequency monitoring error is within 0.01 Hz. This experimental result further validates the effectiveness of the model proposed in this paper.

From Table 2, it can be seen that the model proposed in this paper has a significant advantage in accuracy. Other models often use a single monitoring method for

monitoring the dancing of transmission lines, while the model proposed in this paper uses a fusion method for monitoring the dancing of transmission lines, resulting in higher accuracy and reducing the monitoring error of the system proposed in this paper and the response time of the system in this article is shorter compared to existing research, which can better meet the practical needs of transmission line monitoring.

The system in this article adopts an embedded mode to construct the hardware framework, so the model in this article has good scalability and can be applied to intelligent monitoring of power systems. Compared with existing models, it has the advantage of scalability. In addition, the chip and monitoring system selected in this article, combined with the communication network, can be extended in existing network systems, effectively reducing the cost of building the basic system structure. Finally, the model presented in this article demonstrates high accuracy in monitoring the dancing of transmission lines, indicating a certain advantage in terms of accuracy compared to existing research.

Through the above analysis, we can know that when the line is covered with ice, the sensitivity of the ice-covered area to the external temperature change is obviously lower than that of the non-ice-covered area, and it can be used as a criterion to locate the area with a higher risk of icing. Theoretically, the equivalent icing thickness of the transmission line can be monitored by using both strain and natural frequency. The characteristics of line galloping and breeze vibration and the feasibility of using distributed optical fibre monitoring are analysed by simulation, and the characteristics of fluctuating wind speed are simulated to correct wind speed. The results show that the frequency is within the monitoring range of multi-parameter distributed optical fibre equipment. Moreover, the simulation shows that the vibration frequency can be reflected by analysing the strain change inside the cable, and it is feasible to use distributed optical fibre to monitor galloping and breeze vibration. Then, experiments of breeze vibration and galloping are carried out in the laboratory. The results show that the time-domain curve of the cable vibration area will appear zigzag characteristics, and the peak value will appear after the sliding difference, which can be used as a criterion to locate the vibration area. The positioning accuracy of galloping and breeze vibration within 60km of the cable is ± 50 m. In addition, spectrum analysis shows that when the cable galloping and breeze vibration, the spectrum curve obtained by distributed optical fibre monitoring will have a peak value at its actual vibration frequency and its multiple frequency doublers. The monitoring error of galloping frequency and breeze vibration frequency is within 0.01 Hz. Therefore, the wind speed measurement is carried out on the actual line in this paper to formally verify the effectiveness of the equipment in monitoring wind vibration.

5 Conclusions

Starting from the basic principles of distributed optical fibres and measurable physical quantities, this paper uses the method of combining theoretical analysis and simulation modelling to establish the mathematical and physical models and signal characteristic models of the multi-dimensional physical quantities (temperature, strain, vibration and light polarisation state) of distributed optical fibre monitoring and line icing and wind vibration events. Moreover, this paper constructs a multi-parameter distributed optical fibre sensing system according to the monitoring requirements, which solves the problem

of low signal-to-noise ratio in long-distance monitoring. In addition, this paper analyses the characteristics of line galloping and breeze vibration and the feasibility of using distributed optical fibre monitoring, and simulates the characteristics of fluctuating wind speed to correct wind speed. The results show that the frequency is within the monitoring range of the multi-parameter distributed optical fibre equipment, and the simulation results show that the vibration frequency can be reflected by analysing the strain changes inside the cable, and it is feasible to use distributed optical fibre to monitor galloping and breeze vibration.

In addition, multi-parameter distributed optical fibre can also be applied in other aspects such as real-time calculation of the maximum current carrying capacity of the line, so the new application scenarios of distributed optical fibre in the field of transmission line safety monitoring need to be further explored.

This article has completed the hardware circuit design, dance algorithm design, IoT wireless communication design, environmental adaptability design, and dance monitoring system installation structure design of the dance monitoring system. There are also areas that need further improvement and optimisation in this study:

1 The environmental adaptability design scheme needs to be further improved. Firstly, it is necessary to conduct relevant experiments on the hardware circuit design and environmental adaptability design of the monitoring system in a real environment to verify whether the monitoring system can effectively avoid external environmental interference. At the same time, it is necessary to further improve the relevant experiments on data transmission of the internet of things in strong electromagnetic environments, and verify the accuracy and integrity of its data transmission.

2 For the extraction algorithm of dancing feature parameters, further optimisation of the algorithm is considered to better obtain the feature parameters of wire dancing. The current experimental results obtained were obtained under laboratory conditions. Subsequently, corresponding experiments need to be conducted on transmission lines in a real environment to verify the accuracy and stability of the system. Based on the specific results, the dance monitoring system will be further optimised and improved to meet the actual engineering needs.

Acknowledgements

Supported by the Science and Technology Project of State Grid Sichuan Electric Power Company, the fund project name is Research on Communication, Protection, and Stability Control Coupling Simulation Analysis Technology Based on Regulation Cloud (521911230001).

References

Brettschneider, S. and Fofana, I. (2021) 'Evolution of countermeasures against atmospheric icing of power lines over the past four decades and their applications into field operations', *Energies*, Vol. 14, No. 19, pp.6291–6298.

Chen, Y., Fan, J., Deng, Z., Du, B., Huang, X. and Gui, Q. (2020a) 'PR-KELM: icing level prediction for transmission lines in smart grid', *Future Generation Computer Systems*, Vol. 102, No. 2, pp.75–83.

Chen, Y., Li, P., Ren, W., Shen, X. and Cao, M. (2020b) 'Field data-driven online prediction model for icing load on power transmission lines', *Measurement and Control*, Vol. 53, Nos. 1–2, pp.126–140.

Ciesielka, W., Gołaś, A., Szopa, K., Bąchorek, W., Benesz, M., Kot, A., … and Zydroń, P. (2020) 'Reliability improvement of power distribution line exposed to extreme icing in Poland', *Bulletin of the Polish Academy of Sciences. Technical Sciences*, Vol. 68, No. 5, pp.1113–1125.

Dong, B., Jiang, X. and Yin, F. (2022) 'Development and prospect of monitoring and prevention methods of icing disaster in China power grid', *IET Generation, Transmission & Distribution*, Vol. 16, No. 22, pp.4480–4493.

Han, X., Sun, P., Xing, B., Wang, J. and Jiang, X. (2022) 'Influence of torsion on icing process of transmission lines', *IET Generation, Transmission Distribution*, Vol. 16, No. 20, pp.4230–4238.

He, S., Song, Y., Huang, H., He, Y., Zhou, S. and Gao, Z. (2024) 'Meteorological characteristics of a continuous ice-covered event on ultra-high voltage transmission lines in Yunnan region in 2021', *Atmosphere*, Vol. 15, No. 4, pp.389–402.

Huang, G., Yan, B., Guo, Y., Zhang, B. and Wu, G. (2023) 'Experimental study on dynamic response characteristics of isolated-span transmission lines after ice-shedding', *High Voltage*, Vol. 8, No. 1, pp.196–208.

Huang, Y., Virk, M.S. and Jiang, X. (2020) 'Study of wind flow angle and velocity on ice accretion of transmission line composite insulators', *IEEE Access*, Vol. 8, No. 1, pp.151898–151907.

Li, B., Bai, J., He, J., Ding, C., Dai, X., Ci, W., … and Yuan, Y. (2023) 'A review on superhydrophobic surface with anti-icing properties in overhead transmission lines', *Coatings*, Vol. 13, No. 2, pp.301–312.

Ma, Y., Pan, H., Qian, G., Zhou, F., Ma, Y., Wen, G., … and Li, T. (2022) '[Retracted] Prediction of transmission line icing using machine learning based on GS-XGBoost', *Journal of Sensors*, Vol. 2022, No. 1, pp.2753583–2753595.

Shen, H., Wan, B., Zhou, S., Kang, J., Chen, H. and Gao, Z. (2023) 'The synoptic characteristics of icing events on transmission lines in Southern China', *Atmosphere*, Vol. 14, No. 12, pp.1789–1800.

Sun, J., Zhang, Z., Li, Y., Yan, Z., Zhai, T., Li, L. and Xiao, Z. (2021) 'Distributed transmission line ice-coating recognition system based on BOTDR temperature monitoring', *Journal of Lightwave Technology*, Vol. 39, No. 12, pp.3967–3973.

Wang, B., Ma, F., Ge, L., Ma, H., Wang, H. and Mohamed, M.A. (2020) 'Icing-EdgeNet: a pruning lightweight edge intelligent method of discriminative driving channel for ice thickness of transmission lines', *IEEE Transactions on Instrumentation and Measurement*, Vol. 70, No. 2, pp.1–12.

Wang, F., Lin, H. and Ma, Z. (2024) 'Transmission line icing prediction based on dynamic time warping and conductor operating parameters', *Energies*, Vol. 17, No. 4, pp.945–955.

Wang, L., Chen, Z., Zhang, W., Lu, Z., Cheng, Y., Qu, X., … and Yang, Y. (2023) 'The causes and forecasting of icing events on power transmission lines in Southern China: a review and perspective', *Atmosphere*, Vol. 14, No. 12, pp.1815–1825.

Weng, B., Gao, W., Zheng, W. and Yang, G. (2021) 'Newly designed identifying method for ice thickness on high-voltage transmission lines via machine vision', *High Voltage*, Vol. 6, No. 5, pp.904–922.

Yang, L., Chen, J., Hao, Y., Li, L., Lin, X., Yu, L., … and Yuan, Z. (2023) 'Experimental study on ultrasonic detection method of ice thickness for 10 kV overhead transmission lines', *IEEE Transactions on Instrumentation and Measurement*, Vol. 72, No. 3, pp.1–10.

Yang, L., Hu, Z., Nian, L., Hao, Y. and Li, L. (2022) 'Prediction on freezing fraction and collision coefficient in ice accretion model of transmission lines using icing mass growth rate', *IET Generation, Transmission & Distribution*, Vol. 16, No. 2, pp.364–375.

Zhang, C., Gong, Q.W. and Koyamada, K. (2020) 'Visual analytics and prediction system based on deep belief networks for icing monitoring data of overhead power transmission lines', *Journal of Visualization*, Vol. 23, No. 4, pp.1087–1100.

Zhang, Z., Zhang, H., Yue, S. and Zeng, W. (2023) 'A review of icing and anti-icing technology for transmission lines', *Energies*, Vol. 16, No. 2, pp.601–611.

Zhou, R., Zhang, Z., Zhai, T., Gu, X., Cao, H., Xiao, Z. and Li, L. (2023) 'Machine learning-based ice detection approach for power transmission lines by utilizing FBG micro-meteorological sensors', *Optics Express*, Vol. 31, No. 3, pp.4080–4093.